Hindawi Publishing Corporation
Journal of Nanomaterials
Volume 2015, Article ID 831065, 8 pages
http://dx.doi.org/10.1155/2015/831065

Research Article

Photoinduced Electron Spin Resonance Phenomenon in α-Cr_2O_3 Nanospheres

S. Khamlich,[1,2] V. V. Srinivasu,[1,2] A. Konkin,[1,2,3] N. Cingo,[1,2,4] F. T. Thema,[1,2] A. Benyoussef,[1,2] and M. Maaza[1,2]

[1] *UNESCO Africa Chair in Nanosciences & Nanotechnology, College of Graduate Studies, University of South Africa, Muckleneuk Ridge, P.O. Box 392, Pretoria, South Africa*
[2] *Nanosciences African Network (NANOAFNET), iThemba LABS-National Research Foundation, 1 Old Faure Road, Somerset West 7129, P.O. Box 722, Somerset West, Western Cape, South Africa*
[3] *Institute for Micro- and Nanotechnologies, Ilmenau University of Technology, Gustav-Kirchhoff Street 7, P.O. Box 100565, 98693 Ilmenau, Germany*
[4] *National Laser Centre, Council for Scientific and Industrial Research, P.O. Box 395, Pretoria 0001, South Africa*

Correspondence should be addressed to S. Khamlich; skhamlich@gmail.com

Received 2 August 2014; Revised 3 December 2014; Accepted 12 December 2014

Academic Editor: Takuya Tsuzuki

The photoinduced phenomenon in α-Cr_2O_3 nanoscaled spherical particles was investigated in the temperature range of 150 up to 315 K. An X-band electron-spin resonance spectrometry was employed to probe the magnetic behavior in α-Cr_2O_3 under an IR illumination in the nanosecond regime. The photoinduced effect on both low and high field ESR signals appears above 280 K and is remarkably enhanced just below Néel temperature T_N. Such a photoinduced ESR phenomenon disappears in a reproducible way in the paramagnetic insulating state which occurs above T_N of crystalline α-Cr_2O_3. In the antiferromagnetic phase, that is, below T_N, the shift of the low field absorption could be attributed to the interaction of the light with specific Cr^{3+} ions located in strongly distorted sites correlated to strong ligand-field effect.

1. Introduction

Photoinduced phenomena including phase transition and surface photoactivation are becoming a hot topic in the light-matter interaction domain and are of a specific interest both from fundamental and technological viewpoints [1–11]. Such a multidisciplinary trend is unlocking new perspectives that allows manipulation of the materials' properties by photons in a tunable way [1]. Some studies have been reported in charge transfer complexes [2], halogen bridged metal complexes [3], and perovskite type oxides [4–6]. A singular specificity to these photoinduced phenomena is their electronic dynamic in the ultrafast temporal regime in various spectral ranges.

In the UV range, Takesada et al. [12] have observed a significant enhancement in the ferroelectric properties in quantum paraelectric oxides. As reported by Mochizuki et al. [13], when MgO and rutile TiO_2 are irradiated with ultraviolet laser light ($\lambda = 325$ nm) in vacuum, their photoluminescence spectra change notably in intensity and in spectral structure with increasing irradiation time. By irradiation with the same laser light at room temperature in O_2 gas, their original photoluminescence reappears. It was concluded that such reversible photoinduced phenomena are results of light-induced oxygen surface desorption/adsorption. Unlike previously reported transient photoinduced effects in manganites, Smolyaninov et al. [14] have observed permanent reflectivity changes following local sample illumination with 488 nm light in charge-ordered $Bi_{0.3}Ca_{0.7}MnO_3$. This was found to be correlated to charge-transfer transitions between oxygen 2p and Mn 3d states. These transitions induce strong perturbations into the periodic arrangement of the Mn^{3+} and Mn^{4+} ions in the charge-ordered state. It was proposed that this photoinduced disorder may lead to charge-order

domain switching and causes a domain wall formation as the ones observed in doped $BaTiO_3$ and $LiNbO_3$ perovskite-type oxides which exhibit a pronounced photorefractive effect [15]. The singular observation of Smolyaninov et al. in $Bi_{0.3}Ca_{0.7}MnO_3$ indicates that photonic band-gap structures may be created using holographic recording in manganites. Recently, Mochizuki and Fujishiro [16] reported the first photoinduced photoluminescence in CeO_2 in both its bulk and nanoscaled forms due to O photoreduction. Such a photoreduction is accompanied by both a valence number change of cerium ions ($Ce^{4+} \rightarrow Ce^{3+}$) and oxygen-defect formation, a process which could be applied to light control of the oxygen-storage and oxygen-release processes at metal-oxide surfaces.

In the IR spectral range, these photoinduced phenomena in simple and multioxides have a unique specificity to either induce, among others, photo-magnetic effects and/or to appear inultrafast phase transitions based systems, in particular in strongly correlated materials. Firstly, the photo-induced magnetism which is generally triggered by a spin crossover inter-conversion and known as light-induced excited spin state trapping is of an appealing interest for magneto-optical technological applications, like optical data storage and fast processing devices. As a typical example, specifically nanoscaled spinel ferrites $Al_{0.2}Ru_{0.8}Fe_2O_4$ systems by Kanki et al. [17] were found to exhibit a cluster-glass behavior near room temperature with the spin-freezing state under illumination. This latter glass spin-freezing was considered as originating from randomness in the local magnetic anisotropy. The additional ultrafast spectroscopic measurements using femtosecond laser excitation indicated that such a photoinduced magnetization was correlated to intervalence charge transfer between mixed valence ions which lead to the change of local magnetic anisotropy and responsibility to applied magnetic fields. The low saturation magnetization under 0.6 μB/unit cell and good conductivity accompanied with a high spin polarized electron level over 75% attribute to this spinel ferrites family an attractive spintronic technological applications. In this photoinduced solid state phenomenon, one should single out the case of the standard yet controversial oxide VO_2 which exhibits a pure 1st order phase transition. Indeed, as reported recently by various authors, the photoinduced phase transition by femtosecond laser pulses in VO_2 has allowed shedding light not only on the so long disputed nature of the transition itself, distinguishing hence the Mott–Hubbard-like transition from the electron trapping in homopolar bonds, but also on its dynamic and the duration of the phase transition itself which was found to be of about 180 fs [18, 19]. The additional complementary recent work of Lysenko et al. [20] indicated that, upon a laser excitation, an instantaneous response in the transient reflectivity and transmission was observed followed by a relatively longer relaxation process. This photoinduced 1st order phase transition characteristic of VO_2 at about 68°C makes it an optical coating candidate of choice for ultrafast optical switching devices [21], field effect transistors, and electrooptical gates [22] as well as ultrafast tunable nanoplasmonics among others [23, 24] as well as optical limiting in the IR spectral region [11].

Another singular oxide is chromium (III) oxide, Cr_2O_3, which is considered in this communication, is of a major importance equivalent to VO_2 [25], and is even superior in view of the magnetic aspect. Indeed, Cr_2O_3 was one of the first oxides which was demonstrated to exhibit specific magnetoelectric characteristics. These properties of Cr_2O_3 are of fundamental interest and have been investigated for their broad potential for technological applications. Following the theoretical calculations by Landau and Lifshitz that the magnetoelectric response is only allowed in media without time-reversal symmetry or inversion symmetry [25], Dzyaloshinskii predicted that Cr_2O_3 should be a magnetoelectric crystal [26]. Based on its magnetic point group, the linear-induced magnetization by an external electric field [27, 28] and the inverse effect [29] were measured experimentally. Such a linear magnetoelectric effect can be decoupled into three contributions, namely, electronic (frozen-ion), ionic (lattice-mediated), and strain-mediated responses [30]. Each term can be further subdivided into spin and orbital contributions. The early ab initio studies were focused on the spin-lattice [31] and spin-electronic [32] terms. First-principles methods have only recently been developed to calculate the full magnetoelectric response tensor, including both spin and orbital contributions [33]. In the case of Cr_2O_3, the spin-lattice term is dominant [32]. More precisely, Íñiguez has shown [31] that the lattice contribution can be written as a product of the Born charge, the force-constant inverse, and the dynamical magnetic charge, which is the magnetic analog of the dynamical Born charge. These magnetoelectric theoretical studies in Cr_2O_3 have been refined recently by Ye and Vanderbilt [34] using first-principles density functional methods to study the dynamical magnetic charges driven by the spin-orbital coupling mechanism.

The current quest for materials, which can be controlled by light illumination to enhance their electronic, magnetic, and structural properties [35–39], leads to the study of the light-induced effect in Cr_2O_3 polycrystalline thin films by Sasaki et al. [40]. They reported the first photoinduced results demonstrating crystal-clearly a light induced enhanced electron spin resonance (ESR) response in 2D type thin films. In this work, complementary to Sasaki et al.'s on 2D films, we investigate the photoinduced ESR phenomena and their temperature evolution in nonagglomerated and quasimonodisperse α-Cr_2O_3 nanospheres using a pulsed Nd-YAG laser ($\lambda \sim 1064$ nm) as an illumination exciting source in the temperature range of 150–315 K.

2. Experiments, Results, and Discussion

The synthesis of α-Cr_2O_3 nanospheres was performed with reagent grade chemicals. The general methodology is described in previous contributions [41, 42] and illustrated in Figure 1(a). An aqueous solution (MilliQ, 18.2 MΩ) of 1 mM of chromium potassium sulfate dodecahydrate ($KCr(SO_4)_2{\cdot}12H_2O$) mixed with polyvinylpyrrolidone (PVP) as a stabilizer in a glass bottle with an autoclavable screw cap was heated in a standard laboratory oven at a constant temperature of about 75°C. Subsequently, the green precipitates of $Cr_2O_3{\cdot}nH_2O$ were formed onto quartz glass and

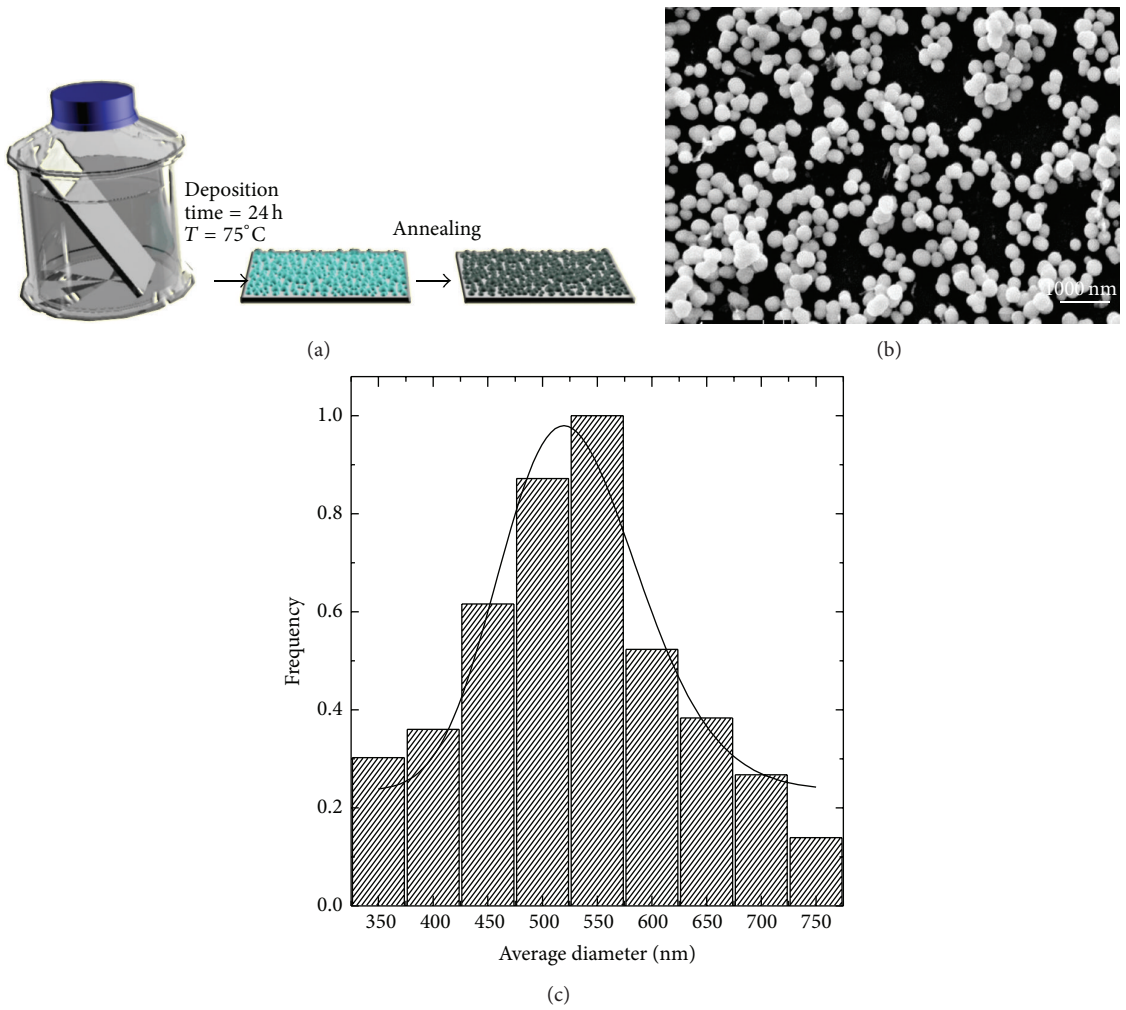

FIGURE 1: (a) Illustration of the synthesis methodology of α-Cr_2O_3 spherical nanoparticles, (b) their typical scanning electron microscopy image, and (c) their corresponding particle size distribution with a log-log simulation.

silicon substrates. The precipitates onto substrates were heat-treated at about 500°C in air, based on the thermal analysis data, for about 1 h to obtain α-Cr_2O_3 spherically shaped particles. The crystalline structure of the spherical particles of α-Cr_2O_3 was investigated using an X-ray diffractometer (XRD, model Bruker AXS D8 Advance, Kα line of copper λ = 1.5406 Å). Their structural characterization was investigated using Raman spectroscopy (Horiba Jobin Yvon, LabRAM HR UV/Vis/NIR) and a Perkin Elmer Spectrum ATR-FTIR with a diamond ATR accessory. Their morphology was investigated using a Leo-StereoScan 440 scanning electron microscope (SEM). The photoinduced phenomenon of the α-Cr_2O_3 nanospheres was investigated using an X-band ($\nu \approx 9.75$ GHz) electron-spin resonance (ESR) spectrometer under an external illumination of a 160 mW Nd:YAG laser operating at its fundamental regime that is with a wavelength $\lambda \sim 1064$ nm and a pulse repetition frequency of ~30 Hz.

Figure 1(b) reports a typical SEM image of the synthesized chromium oxide particles. It demonstrates that isolated spherical chromium oxide particles can be produced with well-defined surface morphology, relatively narrow size distribution, and a prominent shape control. Figure 1(c) shows the corresponding particle size distribution histogram. The ordinate indicates the frequency, which is normalized as number of particles with $\langle \emptyset \rangle$/total number of particles. The distribution has a long tail toward larger size particles. The data which was fitted to a log-normal distribution gives a mean diameter of $\langle \emptyset \rangle \sim 527$ nm highlighting the nanoscale aspect of the chromium oxide spheres.

Figure 2 depicts a typical XRD pattern of a film of chromium oxide nanospheres. All observed Bragg peaks coincide with those given in the JCPDS card 74–0326 of the bulk α-Cr_2O_3. More precisely, these Bragg peaks are attributed to the rhombohedral structure (space group $R\bar{3}c$) with unit cell parameters of about $a \sim 4.96070$ and $c \sim 13.59900$ (Å) of pure α-Cr_2O_3 green phase under a slight compressive stress. Hence, these nanoscaled α-Cr_2O_3 would not exhibit a size effect but likely surface ones if any.

Figure 3 reports a typical infrared vibrational spectrum at room temperature obtained using attenuated total reflection (ATR) geometry of the synthesized powder of α-Cr_2O_3 nanospheres. This result reveals two strongest bands centered

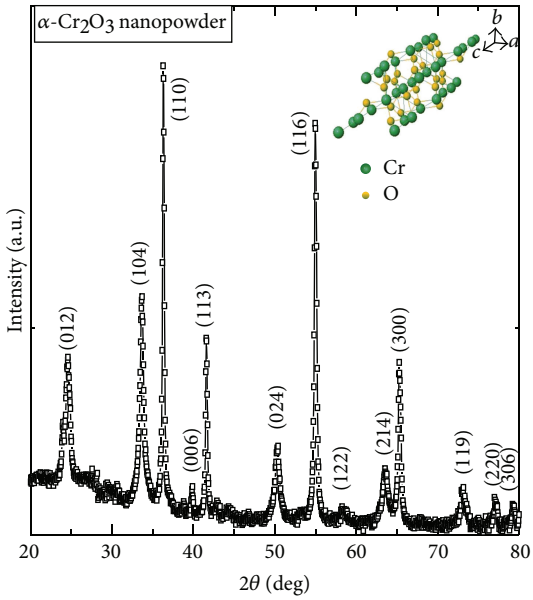

FIGURE 2: Typical room temperature XRD pattern of α-Cr_2O_3 nanospheres with a slight compressive stress.

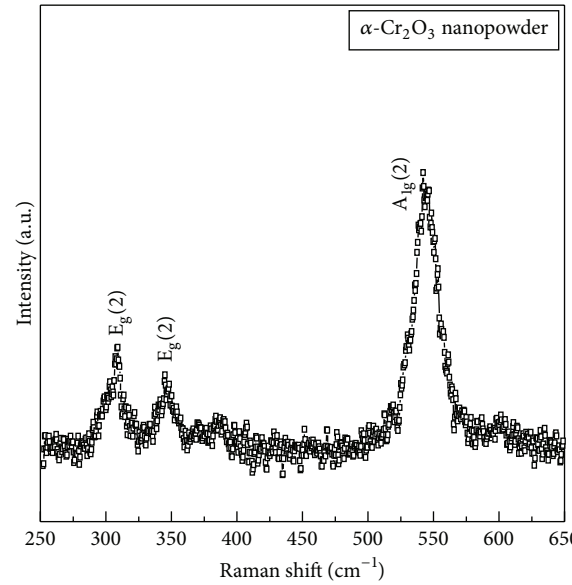

FIGURE 4: Typical room temperature Raman spectroscopy profile of α-Cr_2O_3 nanospheres deposited onto quartz substrate.

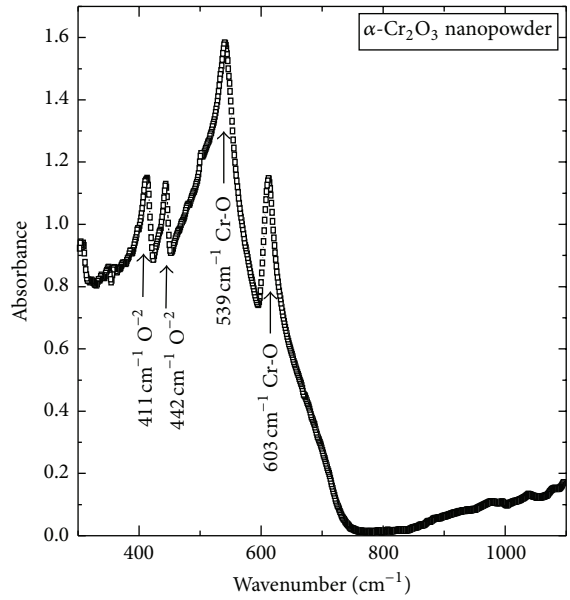

FIGURE 3: Typical room temperature ATR-FTIR pattern of α-Cr_2O_3 nanospheres scrapped from the quartz substrate.

at 539 and 603 cm^{-1}. These values fall well within the range reported in the literature for samples having the adequate α-Cr_2O_3 stoichiometry. Both bands are associated with Cr–O stretching modes (symmetrical stretching and antisymmetrical stretching) in α-Cr_2O_3 and are due to various combinations of O^{2-} and Cr^{3+} displacements in the lattice. The pair of sharp bands at 442 and 411 cm^{-1} corresponds to two specific O^{2-} displacements in the lattice.

Figure 4 reports a typical room temperature Raman spectrum of the α-Cr_2O_3 nanospheres. As one could notice, two E_g and one A_{1g} modes of chromium (III) oxide are observed. As well established, bulk chromium (III) oxide has a corundum structure that belongs to the $D^6{}_{3d}$ space group and consists of a hexagonal close packed array of oxide anions with 2/3 of the octahedral holes occupied by chromium. The site symmetry for the Cr atoms is C_3, whereas the O atoms are on sites having C_2 symmetry. The optical modes in the crystal are $2A_{1g}$, $2A_{1u}$, $3A_{2g}$, $2A_{2u}$, $5E_g$, and $4E_u$ vibrations with only two A_{1g} and five E_g vibrations which are Raman active. As mentioned above, in the present work related to isolated α-Cr_2O_3 nanospheres, it was found, in a reproducible manner on several similar samples that only the two E_g and one A_{1g} modes subsist. The observation of only this set of limited modes cannot be caused by size effects in the α-Cr_2O_3 nanospheres and/or to the breakdown of the 3D symmetry of surface site atoms. Compared to bulk α-Cr_2O_3 material, the shift of the most intense Raman peak, assigned to A_{1g} symmetry, from 533 to 543 cm^{-1}, indicated a significant internal compressive stress which might be related to surface effects, as it was noted in the XRD patterns. As a preliminary conclusion and from the combined XRD, Raman, and IR-ATR results, one could preconclude on the phase purety of α-Cr_2O_3 nanospheres and that there are no substantial size effects but rather surface ones.

Figure 5 reports the electron spin resonance (ESR) profiles with and without IR laser illumination which are the major focus of this short contribution. The investigations were carried out at different temperatures ranging from 150 to 315 K. The solid and dash curves correspond to the ESR profiles in dark that is without laser illumination and under laser illumination, respectively. The observed ESR profiles retain a Lorentzian curvature centered at the high magnetic field resonance of 3440 G. As one can notice, there are two components in fact: a low and a high field component. This first observation of the ESR signature of the α-Cr_2O_3

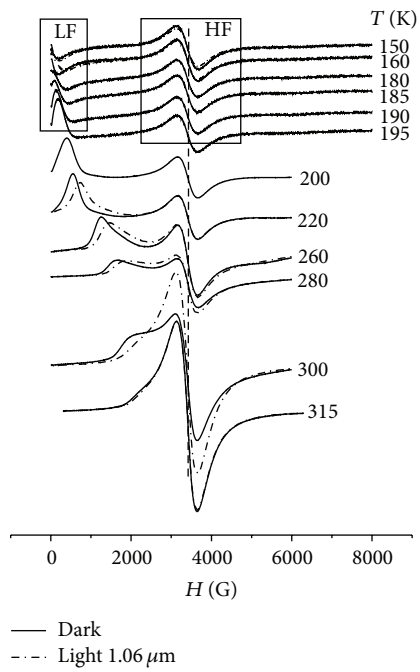

FIGURE 5: ESR profiles without (plan curves) and with (dashed curves) laser illumination of α-Cr_2O_3 nanospheres deposited onto quartz substrate within the temperature range of 150 to 315 K.

nanospheres is in contrast to the pioneering work of Sasaki et al. and Yanagisawa et al. on 2D sputtered thin films where there was only one ESR resonance (the high field one). In addition, one can also distinguish that while the position of the high field ESR absorption does not vary with temperature up to nearly 280 K, the low field component shifts substantially towards high fields. More accurately, the higher is the temperature, the larger is the shift of the low field component. It adds to the high field component near the Neel temperature $T_N \sim 308$ K. While shifting, the low field component becomes broader. Likewise, it is worth mentioning that this shift has not been observed by Sasaki et al. as well as by Yanagisawa et al. in their sputtered 2D thin films.

In terms of the photo-induction phenomenon, and as in the case of Sasaki et al. and Yanagisawa et al, there is no noticeable variation in the high field ESR absorption with the Nd-YAG illumination below 280 K. Above such a temperature up to $T_N \sim 308$ K, the high field ESR absorption is enhanced indeed as in the case of Sasaki et al. and Yanagisawa et al. The enhancement of the ESR absorption at 3440 G is maximum just below T_N and vanishes rapidly above such a critical temperature. Consequentially, this indicates crystal clearly that the photo-induction phenomenon is related to primarily magnetic fluctuations as the magnetic susceptibility presents a singularity at $T_N \sim 308$ K. More precisely, one could conclude that the observed photoinduced enhancement both in our case (α-Cr_2O_3 nanospheres) as well as in the 2D thin films by Sasaki et al. and Yanagisawa et al. is directly related to the antiferromagnetic/paramagnetic phase transition of the α-Cr_2O_3 structure. It is worth noticing that the photoinduction effect starts as early as 220 K for the low field ESR absorption. Hence, the shift of the low field absorption in the antiferromagnetic state of α-Cr_2O_3 can be attributed to the interaction of the light with Cr^{3+} ions in the strongly distorted sites due to strong ligand-field effect. As mentioned before, while the ESR absorption enhancement is likely to be attributed to the magnetic fluctuations in the α-Cr_2O_3, the physical origin of this photoinduced effect could only be related to the Cr^{3+} ions. Cr_2O_3, is a well-known antiferromagnet with magnetic point group symmetry $\bar{3}m$ [43]. Below the Néel temperature $T_N \sim 308$ K, the four chromium spins in the unit cell are aligned along the threefold axis (z-axis) of the crystal in a $+ - + -$ fashion, reducing the magnetic symmetry to $\underline{\bar{3}m}$ [44]. Because of the antiferromagnetic order, the crystal loses both space and time reversal symmetry while the product of the parity operations is still a symmetry operation. Cr_2O_3 exhibit the spontaneous nonreciprocal reflection of light that was predicted several decades ago [45] but first observed on α-Cr_2O_3 [46].

What is the physical origin of such an ESR absorption enhancement and the observed photo-induced effect in the investigated nanoscaled α-Cr_2O_3 spheres? This photoinduced ESR phenomenon could be caused by the peculiar optical properties of Cr^{3+} ions ($3d^3$) in α-Cr_2O_3 that originate from the d-d electronic transitions between the splitted lower triply degenerated t_{2g} levels and the upper doubly degenerated e_g levels of the fivefold degenerated 3d orbitals of the chromium ions in the centrosymmetric D_{3d} point group. The free ions Russell–Saunders coupling in D_{3d} symmetry are ^4F, ^2G, and ^4P. The ground state is ^4F, which splits into $^4A_2$, $^4T_2$, and $^4T_1$. The excited state is ^2G and splits into ^2E, $^2T_1$, $^2T_2$, and $^2A_1$. The optical transitions originate from the strong spin-allowed but parity-forbidden $^4A_{2g} \rightarrow {}^4T_{2g}$ and $^4A_{2g} \rightarrow {}^4T_{1g}$ transitions as well as from the weak spin- and parity-forbidden transitions $^4A_{2g} \rightarrow {}^2E_{2g}$, and $^4A_{2g} \rightarrow {}^2T_{1g}$ [47]. The bandwidths of such transitions are usually large due to the strong electronic coupling to vibrations of the local environment as well as the stoichiometry, size, and surface morphology of the samples. In addition, the observed ESR absorption enhancement and the photoinduced effect can be correlated to the experimental findings of Fiebig et al. [48, 49]. They have observed a strong second harmonic generation signal [49] originating from the $^4A_{2g} \rightarrow {}^4T_{2g}$ transition of Cr^{3+} ions in α-Cr_2O_3 due to the two-photon excitation of $^4T_{2g}$ levels below T_N [48] and have been used to image the antiferromagnetic domains and determine magnetic symmetry. Likewise, it is noteworthy to highlight an analogous observed photoinduced effect by Terakado and Tanaka [50]. They have reported the first studies on photoinduced changes in GeO_2 glass system which has been investigated in terms of its optical and structural properties too. It was found that band-gap excitation gives rise to modifications in midgap optical absorption and photoluminescence spectra, producing electron-spin signals at $g \simeq 1.995$ and 2.008 which were related to photoinduced bond transformations from rutile-like to defective quartz-like structures and/or from small to large rings.

At last, one might suspect that the current observed photoinduced ESR phenomenon in the α-Cr_2O_3 nanospheres is driven by the Nd-YAG laser heating. The evidence against such a hypothesis is provided by the temperature dependence of ESR profiles themselves. As indicated in Figure 5, there is no difference among those profiles at low temperatures where the result is expected to be sensitive for this kind of heating. In fact, the ESR profile after the postmeasurement with the optical excitation shows almost identical with that obtained prior to the optical excitation. From experimental viewpoint, such a photoinduced aspect could be extended to engineer tunable bang gap engineering of core shell oxide/α-Cr_2O_3 nanostructures [51–54].

3. Conclusion

Photoinduced ESR effects and enhancement at high field in α-Cr_2O_3 nanospheres were investigated and observed. It was found that the light-induced ESR signal appears above 280 K in both low and high magnetic fields and is remarkably enhanced just below the vicinity of T_N for the high field ESR absorption resonance. Consequentially, this latter was concluded to be correlated to magnetic fluctuations, specifically at the edge of the antiferromagnetic/paramagnetic phase transition where the magnetic susceptibility exhibits a singularity. Relatively to 2D continuous thin films, the photoinduced ESR absorption resonance of the nonagglomerated nanospheres presents an additional low field component which shifts towards high field values with the increasing of temperature. The present results open up a framework of more detailed future research on the light-induced effect in chromites as well as new possibilities of tunable photoinduced magnetooptical applications in α-Cr_2O_3 based nanoscaled devices. From fundamental viewpoint, this study could reopen the chapter of nonreciprocity. Indeed, the specificity of the magnetoelectric effect in α-Cr_2O_3 is characterized by the spontaneous nonreciprocal optical effects such as the gyrotropic birefringence and dichroism for which time and parity symmetry are broken.

Conflict of Interests

The authors declare that there is no conflict of interests regarding the publication of this paper.

Acknowledgments

This work was sponsored within the framework of the UNESCO UNISA Africa Chair in Nanosciences & Nanotechnology and the Nanosciences African Network (NANOAFNET) by the National Research Foundation of South Africa, the African Laser Centre (ALC), the University of South Arica (UNISA) in collaboration with iThemba LABS, and the Abdus Salam ICTP-Trieste. Likewise, the authors do acknowledge the contribution of the Institute for Micro- and Nanotechnologies, Ilmenau, Germany.

References

[1] K. Nasu, Ed., *Relaxations of Excited States and Photo-Induced Structural Phase Transitions*, vol. 124 of *Springer Series in Solid-State Sciences*, Springer, Berlin, Germany, 1997.

[2] S. Iwai, S. Tanaka, K. Fujinuma, H. Kishida, H. Okamoto, and Y. Tokura, "Ultrafast optical switching from an ionic to a neutral state in tetrathiafulvalene-p-chloranil (TTF-CA) observed in femtosecond reflection spectroscopy," *Physical Review Letters*, vol. 88, no. 5, pp. 574021–574024, 2002.

[3] S. Iwai, M. Ono, A. Maeda et al., "Ultrafast optical switching to a metallic state by photoinduced mott transition in a halogen-bridged nickel-chain compound," *Physical Review Letters*, vol. 91, no. 5, Article ID 057401, 4 pages, 2003.

[4] T. Ogasawara, T. Kimura, T. Ishikawa, M. Kuwata-Gonokami, and Y. Tokura, "Dynamics of photoinduced melting of charge/orbital order in a layered manganite $La_{0.5}Sr_{1.5}MnO_4$," *Physical Review B: Condensed Matter and Materials Physics*, vol. 63, no. 11, Article ID 113105, 2001.

[5] M. Fiebig, K. Miyano, Y. Tomioka, and Y. Tokura, "Sub-picosecond photo-induced melting of a charge-ordered state in a perovskite manganite," *Applied Physics B: Lasers and Optics*, vol. 71, no. 2, pp. 211–215, 2000.

[6] S. Tomimoto, S. Miyasaka, T. Ogasawara, H. Okamoto, and Y. Tokura, "Ultrafast photoinduced melting of orbital order in $LaVO_3$," *Physical Review B*, vol. 68, Article ID 035106, 2003.

[7] E. Collet, M.-H. Lemée-Cailleau, M. B.-L. Cointe et al., "Laser-induced ferroelectric structural order in an organic charge-transfer crystal," *Science*, vol. 300, no. 5619, pp. 612–615, 2003.

[8] M. Nakajima, K. Kazumi, M. Isobe, Y. Ueda, and T. Suemoto, "Time-resolved Raman spectroscopy applied to the photoinduced phenomena in NaV_2O_5," *Journal of Physics: Conference Series*, vol. 21, pp. 201–206, 2005.

[9] B. D. Ngom, O. Sakho, S. Ndiaye et al., "Photon-induced tunable and reversible wettability of pulsed laser deposited W-doped ZnO nanorods," *The European Physical Journal: Applied Physics*, vol. 55, no. 2, Article ID 20501, 2011.

[10] S. Khamlich, O. Nemraoui, N. Mongwaketsi, R. McCrindle, N. Cingo, and M. Maaza, "Black Cr/α-Cr_2O_3 nanoparticles based solar absorbers," *Physica B: Condensed Matter*, vol. 407, no. 10, pp. 1509–1512, 2012.

[11] M. Maaza, D. Hamidi, A. Simo, T. Kerdja, A. K. Chaudhary, and J. B. Kana Kana, "Optical limiting in pulsed laser deposited VO_2 nanostructures," *Optics Communications*, vol. 285, no. 6, pp. 1190–1193, 2012.

[12] M. Takesada, T. Yagi, M. Itoh, T. Ishikawa, and S. Koshihara, "Photoinduced phenomena in quantum paraelectric oxides by ultraviolet laser irradiation," *Ferroelectrics*, vol. 298, no. 1, pp. 317–323, 2004.

[13] S. Mochizuki, F. Fujishiro, A. Iino, K. Shibata, and H. Yamamoto, "Photo-induced defects of metal oxides: MgO and rutile TiO_2," *Physica B: Condensed Matter*, vol. 401-402, pp. 426–429, 2007.

[14] I. I. Smolyaninov, V. N. Smolyaninova, C. C. Davis, B.-G. Kim, S.-W. Cheong, and R. L. Greene, "High resolution study of permanent photoinduced reflectivity changes and charge-order domain switching in $Bi_{0.3}Ca_{0.7}MnO_3$," *Physical Review Letters*, vol. 87, no. 12, Article ID 127204, 2001.

[15] D. G. Choi, S. R. Kim, and S. K. Choi, "Nonsteady-state photovoltaic current and photoinduced domain switching in poled $(Pb_{0.85}La_{0.15})TiO_3$ and $BaTiO_3$ ferroelectric ceramics,"

Japanese Journal of Applied Physics, vol. 38, no. 3, part 1, pp. 1394–1397, 1999.

[16] S. Mochizuki and F. Fujishiro, "The photoluminescence properties and reversible photoinduced spectral change of CeO_2 bulk, film and nanocrystals," *Physica Status Solidi B: Basic Research*, vol. 246, no. 10, pp. 2320–2328, 2009.

[17] T. Kanki, Y. Hotta, N. Asakawa, M. Seki, H. Tabata, and T. Kawai, "Room-temperature-photoinduced magnetism and spin-electronic functions of spinel ferrite with a spin-cluster structure," *Applied Physics Letters*, vol. 92, no. 18, Article ID 182505, 2008.

[18] A. Cavalleri, C. Toth, C. W. Siders, J. Squier, F. Raski, and J. Kieffer, "Femtosecond structural dynamics in VO_2 during an ultrafast solid-solid phase transition," *Physical Review Letters*, vol. 87, Article ID 237401, 2001.

[19] A. Cavalleri, T. Dekorsy, H. H. W. Chong, J. C. Kieffer, and R. W. Schoenlein, "Evidence for a structurally-driven insulator-to-metal transition in VO_2: a view from the ultrafast timescale," *Physical Review B—Condensed Matter and Materials Physics*, vol. 70, no. 16, Article ID 161102, 2004.

[20] S. Lysenko, A. J. Rua, V. Vikhnin, J. Jimenez, F. Fernandez, and H. Liu, "Light-induced ultrafast phase transitions in VO_2 thin film," *Applied Surface Science*, vol. 252, no. 15, pp. 5512–5515, 2006.

[21] J. B. K. Kana, J. M. Ndjaka, G. Vignaud, A. Gibaud, and M. Maaza, "Thermally tunable optical constants of vanadium dioxide thin films measured by spectroscopic ellipsometry," *Optics Communications*, vol. 284, no. 3, pp. 807–812, 2011.

[22] I. Balberg and S. Trokman, "High-contrast optical storage in VO_2 films," *Journal of Applied Physics*, vol. 46, no. 5, pp. 2111–2119, 1975.

[23] M. Maaza, C. Sella, B. Baruch-Barak, O. Nemraoui, and A. C. Beye, "Thermal induced tunability of surface plasmon resonance in Au-VO_2 nano-photonics," *Optics Communications*, vol. 254, no. 1–3, pp. 188–195, 2005.

[24] M. Maaza, O. Nemraoui, C. Sella, and A. C. Beye, "Surface plasmon resonance tunability in Au-VO_2 thermochromic nanocomposites," *Gold Bulletin*, vol. 38, no. 3, pp. 100–106, 2005.

[25] L. D. Landau and E. M. Lifshitz, *Electrodynamics of Continuous Media: Course of Theoretical Physics*, vol. 8, Pergamon Press, Oxford, UK, 1960.

[26] I. E. Dzyaloshinskii, "On the magneto-electrical effect in antiferromagnets," *Soviet Physics*, vol. 10, pp. 628–629, 1960, *Zhurnal Eksperimental'Noi I Teoreticheskoi Fiziki*, vol. 37, no. 3, pp. 881–882, 1959.

[27] D. N. Astrov, "The magnetoelectric effect in antiferromagnetics," *Journal of Experimental and Theoretical Physics*, vol. 38, pp. 984–985, 1960.

[28] V. J. Folen, G. T. Rado, and E. W. Stalder, "Anisotropy of the magnetoelectric effect in Cr_2O_3," *Physical Review Letters*, vol. 6, no. 11, pp. 607–608, 1961.

[29] G. T. Rado and V. J. Folen, "Observation of the magnetically induced magnetoelectric effect and evidence for antiferromagnetic domains," *Physical Review Letters*, vol. 7, no. 8, pp. 310–311, 1961.

[30] T. Birol, N. A. Benedek, H. Das et al., "The magnetoelectric effect in transition metal oxides: Insights and the rational design of new materials from first principles," *Current Opinion in Solid State and Materials Science*, vol. 16, no. 5, pp. 227–242, 2012.

[31] J. Íñiguez, "First-principles approach to lattice-mediated magnetoelectric effects," *Physical Review Letters*, vol. 101, no. 11, Article ID 117201, 4 pages, 2008.

[32] E. Bousquet, N. A. Spaldin, and K. T. Delaney, "Unexpectedly large electronic contribution to linear magnetoelectricity," *Physical Review Letters*, vol. 106, no. 10, Article ID 107202, 4 pages, 2011.

[33] A. Malashevich, S. Coh, I. Souza, and D. Vanderbilt, "Full magnetoelectric response of Cr_2O_3 from first principles," *Physical Review B*, vol. 86, Article ID 094430, 2012.

[34] M. Ye and D. Vanderbilt, "Dynamical magnetic charges and linear magnetoelectricity," *Physical Review B*, vol. 89, no. 6, Article ID 064301, 7 pages, 2014.

[35] J. B. Goodenough, *Metallic Oxides*, Edited by: H. Reiss, Pergamon Press, Oxford, UK, 1971.

[36] K. Miyano, T. Tanaka, Y. Tomioka, and Y. Tokura, "Photoinduced insulator-to-metal transition in a perovskite manganite," *Physical Review Letters*, vol. 78, no. 22, pp. 4257–4260, 1997.

[37] Y. Shen, T. Nakayama, M. Arai, O. Yanagisawa, and M. Izumi, "Magnetic phase transition and physical properties of spinel-type nickel manganese oxide," *Journal of Physics and Chemistry of Solids*, vol. 63, no. 6–8, pp. 947–950, 2002.

[38] O. Yanagisawa, M. Izumi, W.-Z. Hu, K.-H. Huang, K. Nakanishi, and H. Nojima, "Evidence of photo-induced melting of the charge-ordered state in $Pr_{0.65}Ca_{0.35}MnO_3$ by X-ray diffraction," *Physica B: Condensed Matter*, vol. 271, no. 1–4, pp. 235–241, 1999.

[39] O. Yanagisawa, M. Izumi, K. H. Huang et al., "Magnetic transitions in thin films of $La_{0.67}Ca_{0.33}MnO_3$ and $Pr_{0.65}Ca_{0.35}MnO_3$," *Journal of Magnetism and Magnetic Materials*, vol. 211, no. 1–3, pp. 254–259, 2000.

[40] S. Sasaki, Y. F. Zhang, O. Yanagisawa, and M. Izumi, "Light-induced ESR in polycrystalline and thin films of Cr_2O_3," *Journal of Magnetism and Magnetic Materials*, vol. 310, no. 2, pp. 1008–1010, 2007.

[41] S. Khamlich, V. V. Srinivasu, O. Nemraoui, R. McCrindle, N. Cingo, and M. Maaza, "Electron spin resonance study of α-Cr_2O_3 and $Cr_2O_3{\cdot}nH_2O$ quasi-spherical nanoparticles," *Nanoscience and Nanotechnology Letters*, vol. 3, no. 4, pp. 550–555, 2011.

[42] L. Vayssieres and A. Manthiram, "2-D mesoparticulate arrays of α-Cr_2O_3," *Journal of Physical Chemistry B*, vol. 107, no. 12, pp. 2623–2625, 2003.

[43] M. Fiebig, D. Fröhlich, and H.-J. Thiele, "Determination of spin direction in the spin-flop phase of Cr_2O_3," *Physical Review B—Condensed Matter and Materials Physics*, vol. 54, no. 18, pp. R12681–R12684, 1996.

[44] M. Fiebig, V. V. Eremenko, and I. E. Chupis, Eds., *Magnetoelectric Interaction Phenomena in Crystals*, Springer, 1st edition, 2004.

[45] R. M. Hornreich and S. Shtrikman, "Theory of gyrotropic birefringence," *Physical Review*, vol. 171, no. 3, pp. 1065–1074, 1968.

[46] B. B. Krichevtsov, V. V. Pavlov, R. V. Pisarev, and V. N. Gridnev, "Spontaneous non-reciprocal reflection of light from antiferromagnetic Cr_2O_3," *Journal of Physics: Condensed Matter*, vol. 5, no. 44, pp. 8233–8244, 1993.

[47] S. Sugano, Y. Tanabe, and H. Kamimura, *Multiplets of Transition Metal Ions in Crystals*, Academic Press, New York, NY, USA, 1970.

[48] M. Fiebig, D. Fröhlich, B. B. Krichevtsov, and R. V. Pisarev, "Second harmonic generation and magnetic-dipole-electric-dipole interference in antiferromagnetic Cr_2O_3," *Physical Review Letters*, vol. 73, no. 15, pp. 2127–2130, 1994.

[49] M. Fiebig, D. Fröhlich, S. Leute, T. Lottermoser, V. V. Pavlov, and R. V. Pisarev, "Determination of magnetic symmetry by optical second-harmonic generation," *Journal of Magnetism and Magnetic Materials*, vol. 226-230, pp. 961–962, 2001.

[50] N. Terakado and K. Tanaka, "Photo-induced phenomena in GeO_2 glass," *Journal of Non-Crystalline Solids*, vol. 352, no. 36-37, pp. 3815–3822, 2006.

[51] R. A. Rakkesh and S. Balakumar, "Facile synthesis of ZnO/TiO_2 core-shell nanostructures and their photocatalytic activities," *Journal of Nanoscience and Nanotechnology*, vol. 13, no. 1, pp. 370–376, 2013.

[52] S. Balakumar and R. A. Rakkesh, "Core/shell nano-structuring of metal oxide semiconductors and their photocatalytic studies," *AIP Conference Proceedings*, vol. 1512, no. 1, pp. 34–37, 2013.

[53] D. Durgalakshmi and S. Balakumar, "Nano-Bioglass (NBG) for bone regeneration applications-preparation and its characterization," in *Proceedings of the 57th DAE Solid State Physics Symposium*, pp. 122–123, December 2012.

[54] P. Parthiban, M. Sakar, and S. Balakumar, "Evolution of silver/gold triangular nanoframes from prismatic silver/gold core/shell nanostructures and their SERS properties," in *Proceedings of the 57th DAE Solid State Physics Symposium*, vol. 1512 of *AIP Conference Proceedings*, pp. 288–289, 2013.